

Rapid, In Situ Detection of *Agrobacterium tumefaciens* Attachment to Leaf Tissue

Christopher W. Simmons

Dept. of Biological and Agricultural Engineering, University of California, Davis, One Shields Avenue, Davis, CA

N. Nitin

Dept. of Biological and Agricultural Engineering, University of California, Davis, One Shields Avenue, Davis, CA

Dept. of Food Science and Technology, University of California, Davis, One Shields Avenue, Davis, CA

Jean S. VanderGheynst

Dept. of Biological and Agricultural Engineering, University of California, Davis, One Shields Avenue, Davis, CA

DOI 10.1002/btpr.1608

Published online August 28, 2012 in Wiley Online Library (wileyonlinelibrary.com).

Attachment of the plant pathogen Agrobacterium tumefaciens to host plant cells is an early and necessary step in plant transformation and agroinfiltration processes. However, bacterial attachment behavior is not well understood in complex plant tissues. Here we developed an imaging-based method to observe and quantify A. tumefaciens attached to leaf tissue in situ. Fluorescent labeling of bacteria with nucleic acid, protein, and vital dyes was investigated as a rapid alternative to generating recombinant strains expressing fluorescent proteins. Syto 16 green fluorescent nucleic acid stain was found to yield the greatest signal intensity in stained bacteria without affecting viability or infectivity. Stained bacteria retained the stain and were detectable over 72 h. To demonstrate in situ detection of attached bacteria, confocal fluorescent microscopy was used to image A. tumefaciens in sections of lettuce leaf tissue following vacuum-infiltration with labeled bacteria. Bacterial signals were associated with plant cell surfaces, suggesting detection of bacteria attached to plant cells. Bacterial attachment to specific leaf tissues was in agreement with known leaf tissue competencies for transformation with Agrobacterium. Levels of bacteria attached to leaf cells were quantified over time post-infiltration. Signals from stained bacteria were stable over the first 24 h following infiltration but decreased in intensity as bacteria multiplied in planta. Nucleic acid staining of A. tumefaciens followed by confocal microscopy of infected leaf tissue offers a rapid, in situ method for evaluating attachment of A. tumefaciens' to plant expression hosts and a tool to facilitate management of transient expression processes via agroinfiltration. © 2012 American Institute of Chemical Engineers Biotechnol. Prog., 28: 1321–1328, 2012

Keywords: Agrobacterium tumefaciens, plant-microbe interaction, nucleic acid stain, confocal microscopy

Introduction

The unique inter-kingdom gene transfer pathway of *Agrobacterium tumefaciens* forms the basis of agroinfiltration, in which the bacteria are used to induce transient expression of transgenes in plant hosts. Agroinfiltration has been extensively used in plant biotechnology and is a promising approach for commercial plant-based production of high-value recombinant proteins^{1,2} and functional characterization of genes in a variety of plant species.^{3,4} Attachment of *A. tumefaciens* to plant cells occurs early in the infection process and is required for successful transgene export to the host plant tissue.⁵ Proximity between bacteria and plant cells is a necessary precursor for attachment. As a result, maximizing contact between *A. tumefaciens* and plant cells is required to achieve optimal transformation efficiencies and

transient expression levels, motivating approaches such as vacuum infiltration, where vacuum application is used to infuse suspensions of *A. tumefaciens* into plant tissues to promote contact with plant cells otherwise isolated within the tissue interior.^{6,7} However, important aspects of vacuum infiltration are not well understood, such as the distribution of attached bacteria within plant tissues following infiltration. Moreover, fundamental aspects of the attachment pathway are poorly understood.^{8,9} Thus, elucidating the attachment behavior of *A. tumefaciens* to plant cells is important for understanding vacuum infiltration and *Agrobacterium*-mediated transformation of plant tissues.¹⁰ There is a need to develop a method to measure *A. tumefaciens* attachment and distribution in plant tissues in order to optimize vacuum infiltration, screen for attachment inhibitors and activators, and understand how initial bacterial attachment relates to plant transformation and *in planta* transient expression of transgenes.

Existing methods for monitoring *A. tumefaciens* attachment to plant tissues require a complimentary technique to

Correspondence concerning this article should be addressed to Jean S. VanderGheynst at jsvander@ucdavis.edu.

address various inadequacies. Present methods rely on plating homogenates of infected plant cells and counting colonies^{11–13} in addition to light and electron microscopy of bacteria bound to plant cells.^{10,11,14–17} Assays based on viable bacterial counts from plated plant homogenates provide no information regarding the distribution of *A. tumefaciens* within plant tissues. Light and electron microscopy are unable to distinguish bacteria that are attached beyond the exposed surface of porous plant tissue samples. Furthermore, preparation of samples for electron microscopy may alter apparent bacterial attachment by disturbing cells.¹⁸ Fluorescence microscopy overcomes many of the drawbacks associated with light and electron microscopy, making it a valuable complimentary technique to these established methods. For instance, bacteria emitting a fluorescent signal can be distinguished from the background in a more reproducible, quantitative fashion compared to light and electron microscopy, where it is largely up to the viewer to determine what elements of an image represent bacteria.

A. tumefaciens expressing green fluorescent protein (GFP) has been used to visualize bacteria bound to a variety of plant tissues and surfaces,^{19,20} but levels of attached bacteria were not quantified. Moreover, prior studies primarily focused on bacteria present on exterior plant surfaces, neglecting how bacteria attach to plant cells of the leaf interior—the most relevant cells for developing transient expression systems in intact plants. Staining of bacteria with fluorescent dyes presents opportunities for quickly labeling cells in lieu of using GFP. However, it is currently unknown if staining affects the native behavior of bacteria. In particular, little is known regarding how fluorescent dyes, specifically those that bind DNA, might affect the infectivity of *A. tumefaciens*, a pathway that critically relies on many proteins interacting with transferred DNA during its export to a host plant cell. Commonly, such DNA-intercalating fluorescent dyes have been used solely to enumerate bacteria in cultures or environmental samples.^{21–25} As such, it is largely unknown if staining affects specific bacterial pathways.

In this study, an imaging method was developed for monitoring *in planta* distribution and levels of attached *A. tumefaciens* under conditions commonly used for plant transformation and induction of transient expression. Three fluorescent staining modalities were investigated: a vital dye, a protein dye, and a dsDNA dye, all with excitation and emission wavelengths chosen to maximize signal-to-background ratio against a leaf background. The stain yielding the greatest signal intensity in bacteria was chosen for imaging *A. tumefaciens* within leaf tissues to examine attachment behavior. To demonstrate the method, labeled bacteria were vacuum infiltrated into lettuce leaf explants and fluorescent confocal microscopy was used to image and quantify labeled *A. tumefaciens* bound to plant cells *in situ* with cellular resolution. Additionally, the effects of staining on bacterial replication and agroinfiltration were examined.

Materials and Methods

Bacterial culture

A. tumefaciens strain C58C1 containing the binary vector pTFS40 was used.²⁶ *A. tumefaciens* C58C1 constitutively expresses virulence genes and does not require chemical induction for virulence. Plasmid pTFS40 from British Sugar Company (Norwich, UK) encodes a T-DNA containing an

intronated β -glucuronidase (GUS) gene driven by the 35S constitutive promoter from cauliflower mosaic virus. Cultures were grown in YEP medium (10 g/L yeast extract, 10 g/L bacto peptone, 5 g/L NaCl) supplemented with 50 mg/L kanamycin, and 5 mg/L tetracycline at 28°C to an optical density of 0.35 at 590 nm, corresponding to $\sim 10^9$ CFU/mL. Cultures were centrifuged at 7000g for 10 min at 4°C and resuspended in sterile water to a density of 10^{10} CFU/mL for staining. For stained cells grown on solid medium, bacteria were diluted to an estimated density of 500 CFU/mL and 50 μ L were plated and grown at 28°C on YEP containing kanamycin and tetracycline with 10 g/L agarose.

Bacterial staining

For stain screening, Syto 16 green fluorescent nucleic acid stain from Invitrogen (Carlsbad, CA), a dsDNA stain; Alexa Fluor 488 carboxylic acid, succinimidyl ester (Alexa 488 CA SE) (Invitrogen), a protein stain; or carboxyfluorescein diacetate succinimidyl ester (CFDA SE), a vital dye from Sigma-Aldrich (St. Louis, MO); was added to resuspended bacteria at a concentration of 10 μ M. For signal intensity studies, Syto 16 was added to resuspended bacteria to achieve concentrations ranging 0–20 μ M. For all stains, cells were incubated with stain for 2 h at room temperature in darkness. Cells were washed three times in sterile water and then suspended in water to a density of 10^9 CFU/mL. For measurements of stain stability, stained bacteria were either incubated in water at room temperature in darkness with no agitation (conditions compatible with maintaining viability but not for rapid growth) or grown in YEP media at 28°C with 150 rpm agitation (conditions conducive to rapid bacterial growth) for 0, 24, 48, and 72 h.

Bacterial infiltration

Lactuca sativa leaf explants were vacuum-infiltrated with suspensions of *A. tumefaciens* using a previously described method.⁷ Leaf explants were vacuum-infiltrated with stained *A. tumefaciens* by submerging them in a suspension of 10^9 CFU/mL stained bacteria and then subjecting them to a pressure of 25 kPa for 7.5 min. Explants were removed from suspension, blotted dry, and then sealed in Petri dishes lined with moistened gauze. The mass of infiltrated bacterial suspension was determined from weight measurements of explants before and after infiltration. For measurement of attached bacteria over time, infiltrated leaf explants were incubated at 22°C in darkness for 0, 24, 48, or 72 h. For measurement of GUS activity in infiltrated leaf tissue, explants were similarly incubated for 72 hours to facilitate transient expression of GUS.

Histochemical staining

GUS expression in leaf tissue was measured via GUS activity as indicated by a histochemical assay.²⁷ Leaf explants were submerged in histochemical staining solution (1 mg/mL 5-bromo-4-chloro-3-indolyl- β -D-glucuronic acid, cyclohexylammonium salt; 10 mM ethylenediaminetetraacetic acid; 0.5 mM potassium ferrocyanide; 0.5 mM potassium ferricyanide; 60 μ L/L Triton X-100, 100 mM sodium phosphate, pH 7.0) and infiltrated in a vacuum chamber at 25 kPa for 5 min. Explants were incubated in staining solution at 37°C for 8 h and then destained with 70% ethanol. Using Adobe Photoshop CS3, 8-bit images of the leaves were converted to

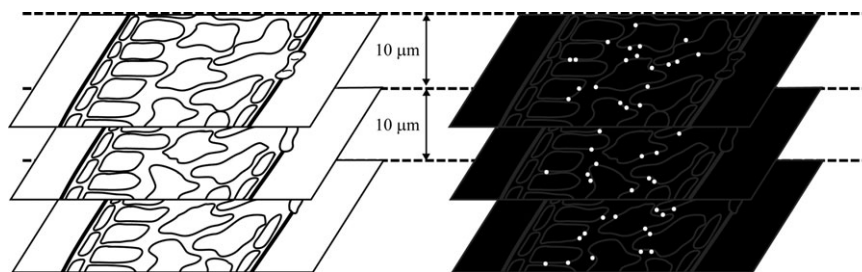


Figure 1. Imaging and analysis of *A. tumefaciens* attachment to leaf tissue at an infection site.

At each infection site, three images of the transverse leaf section were obtained in both brightfield (left stack) and fluorescent confocal (right stack) modes, spanning a total of 20 μm of leaf tissue.

binary using a signal intensity threshold of 100 and the stained areas of leaves were measured.

Sectioning

Leaf explants were sectioned transversely as live, unfixed tissue using a manual vibrating microtome (Leica VT1000P). Sections were 200 μm thick in order to preserve leaf ultra-structure. To remove unattached bacteria, sections were washed in distilled water by gently agitating them in an excess of distilled water using a soft-bristled brush.

Microscopy

An IX71 confocal microscope with spinning disk unit from Olympus (Tokyo, Japan) equipped with an ORCA-ER camera from Hamamatsu Photonics (Hamamatsu, Japan) was used for imaging leaf sections and labeled bacteria in suspension and within leaf tissues. The microscope contained filter cubes for isolating wavelengths associated with common fluorophores: U-N31001 (Chroma Technology, excitation: 480/30 nm (center wavelength/bandwidth), emission: 535/40 nm), U-N31002 (Chroma Technology, excitation: 540/25 nm, emission: 605/55 nm), U-N31023 (Chroma Technology, excitation: 640/20 nm, emission: 680/30 nm), and OSF-0007 (Semrock, excitation: 387/11 nm, emission: 447/60 nm).

For measurements of leaf autofluorescence, washed leaf sections were immediately analyzed after sectioning. Randomly selected locations within sections from noninfiltrated lettuce leaf explants were imaged using fluorescence microscopy. An exposure time of 100 ms was used. For samples of stained bacteria in suspension, 10 μL of suspension containing 10^9 CFU/mL bacteria were placed on poly-L-lysine-coated glass slides. Bacteria at the slide surface were imaged in confocal mode using the U-N31001 filter cube. For washed leaf sections containing attached *A. tumefaciens*, sections were scanned for localizations of attached bacteria, representing infection sites, in fluorescent widefield mode. Three infection sites were imaged for each leaf explant. Three images were taken in both brightfield and fluorescent confocal modes at each infection site, capturing 0, 10, and 20 μm deep into the leaf section. Confocal images were obtained using the U-N31001 filter cube.

Image analysis

Metamorph Basic software (version 7.6.5.0, Olympus) was used for image processing and analysis. For fluorescent micrographs of noninfiltrated leaf tissue, the average 12-bit

intensity across the entire image was calculated as a measure of autofluorescence for each tested pairing of excitation and emission wavelengths. For fluorescent confocal micrographs of bacterial suspensions, 12-bit signal intensity thresholds were selected to isolate signals from bacteria and the mean average 12-bit pixel intensity across all bacteria in each image was measured. For fluorescent confocal micrographs of leaf tissues infiltrated with labeled *A. tumefaciens*, a threshold signal intensity level of 250 on a 12-bit intensity scale was used to exclude most plant tissue autofluorescence and isolate bacterial signals in images. In addition to intensity thresholding, signals from bacterial cells were isolated based on a signal region area filter (signal area between 0.078 μm^2 and 3.9 μm^2) to exclude most artifacts within plant tissues. Signal regions with intensities above the threshold intensity were counted to determine the number of bacterial cells within a given image. The sample volume encompassed by the three images of an infection site was calculated as the leaf section area present in the images, as determined from brightfield images, multiplied by 20 μm , the total depth that the three images spanned (Figure 1). The total number of bacteria present across the three images of an infection site, represented as white dot signals in fluorescent confocal micrographs in Figure 1, was divided by the leaf section sample volume to determine the density of bound bacteria within an infection site (Figure 1). The average density of bound bacteria within a leaf explant was calculated as the average of the densities determined at each of the three sampled infection sites.

Parameter fitting and statistical analysis

The nonlinear fit (nlinfit) function of MATLAB R2009a version 7.8.0.347 from MathWorks (Natick, MA) was used to fit parameters in the saturation model describing signal intensity versus stain concentration. JMP version 8.0 from SAS Institute Inc. (Cary, NC) was used to compare means and test hypotheses. Student's *t*-test and Tukey's Honestly Significantly Different (HSD) test were used to test sample mean differences from hypothesized values.

Results

Selection of optimal imaging wavelengths for leaf tissue based on leaf autofluorescence

Sections of fresh lettuce leaf tissue were imaged using a variety of excitation and emission wavelengths to determine levels of average autofluorescence intensity in leaf samples. Table 1 shows average autofluorescent signal intensity in lettuce leaves for paired sets of excitation and emission

Table 1. Lettuce Leaf Autofluorescence at Various Excitation and Emission Wavelengths

$\lambda_{\text{excitation}}$ (nm)	$\lambda_{\text{emission}}$ (nm)	Average Signal Intensity (12-bit)
387/11	447/60	452.31 (35.11) A
480/30	535/40	270.36 (5.00) A
540/25	605/55	298.44 (7.70) A
640/20	680/30	2096.24 (455.36) B

Average intensity values represent average 12-bit pixel intensities from 40x images of leaf sections imaged using the given excitation and emission wavelengths. Three randomly selected areas of leaf tissue were imaged with each pairing of wavelengths. Wavelengths are given as center wavelength/bandwidth of the filter cube used for imaging. Intensity values are given as the mean with 1 standard deviation in parentheses. Values not connected by the same letter are significantly different ($\alpha = 0.05$).

wavelengths corresponding to common fluorophores for a fixed camera exposure time. The results show that the mean autofluorescence intensity was highest for the red excitation and emission pair (excitation at 640/20 nm and emission at 680/30 nm). Other wavelength combinations did not result in statistically significant differences in average autofluorescence intensity, although the autofluorescence level for the UV excitation and emission pair was higher than the blue and green excitation and emission pairs. In light of these results, excitation and emission wavelengths of 488 nm and 520 nm, respectively, were chosen for the stain fluorophore to provide maximal fluorescence contrast against a leaf background.

Selection of optimal staining approach for bacterial cells

A. tumefaciens was stained with Syto 16 green fluorescent nucleic acid stain to label dsDNA, Alexa 488 CA SE to label surface proteins, or CFDA SE, a vital dye. All stain fluorophores shared the same excitation and emission wavelengths (488 nm and 520 nm, respectively). The mean average signal intensity from bacteria stained with Alexa 488 CA SE was not significantly higher than unstained controls, which had no detectable signals. Bacteria labeled with CFDA SE had a mean average pixel intensity of 254.0 ± 5.3 (± 1 standard deviation, $n = 3$). Bacteria stained with Syto 16 nucleic acid stain exhibited a mean average pixel intensity of 810.6 ± 158.4 (± 1 standard deviation, $n = 3$), significantly higher than bacteria stained with CFDA SE ($P = 0.026$). Based on the signal intensity of stained bacteria, Syto 16 nucleic acid stain was selected for further study. Signal stability in Syto 16-stained bacteria was investigated by measuring signal intensity over time for bacteria stored in water at room temperature or cultured in YEP as described in the methods section. For bacteria stored in water, signal intensities were constant up to 72 h after staining (Figure 2). Alternately, signal intensities in bacteria incubated in media decreased rapidly, with signal intensity dropping $\sim 75\%$ within 6 h following staining, suggesting that the stain was diluted among daughter cells during proliferation.

Optimizing staining concentration

The mean average 12-bit pixel intensity of Syto 16-labeled *A. tumefaciens* was measured in response to varying concentrations of Syto 16 nucleic acid stain during staining (Figure 3). Signal intensity in stained cells exhibited a saturation trend with respect to stain concentration. The trend could be described by a saturation function of the form

$$I = I_{\text{max}}S(S_{1/2} + S)^{-1} \quad (1)$$

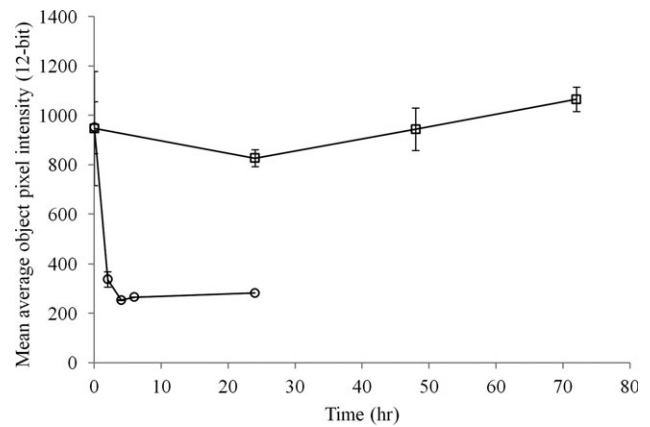


Figure 2. Fluorescent signal stability in Syto 16-stained *A. tumefaciens* incubated in water or media.

Squares and circles represent data from bacteria incubated in water and YEP media, respectively. Values are given as means with error bars representing 1 standard deviation.

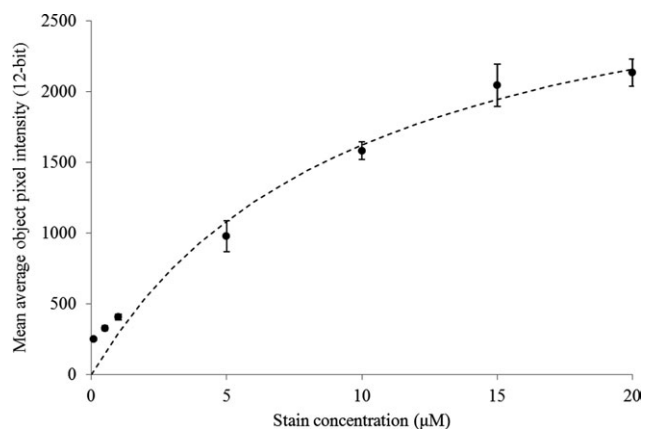


Figure 3. Mean average object pixel intensity in images of *Agrobacterium tumefaciens* stained with Syto 16 versus stain concentration applied.

Values are given as means with error bars representing 1 standard deviation. The dashed line is the fitted saturation model as presented in equation 1.

where I_{max} is the theoretical maximum mean average pixel intensity in stained cells, S is the concentration of stain applied, and $S_{1/2}$ is the stain concentration required for achieving half the theoretical maximum signal intensity in stained cells. Values of I_{max} and $S_{1/2}$ were estimated to be 3227.1 and 9.9 μM , respectively, based on non-linear regression of the data.

Viability and virulence of stained bacteria

Syto 16-labeled bacteria were observed to be motile up to 72 h following staining. Syto 16-labeled and unlabeled suspensions of *A. tumefaciens* were inoculated onto solid media and colony counts were performed to determine the viability of stained bacteria compared to unstained controls. Plates with stained bacteria exhibited 20 ± 3.7 colonies, corresponding to 400 ± 74 CFU/ml in the inoculum (± 1 standard deviation, $n = 5$), and plates with unstained bacteria had 19 ± 5.7 colonies, corresponding to 380 ± 114 CFU/ml in the inoculum (± 1 standard deviation, $n = 5$). There was not a significant difference in viable cell count between stained

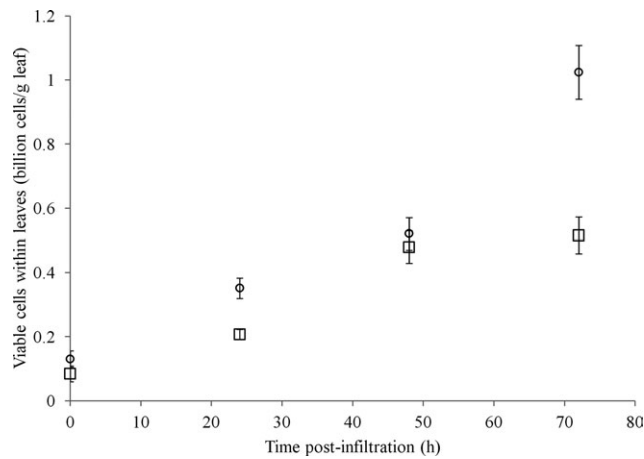


Figure 4. Proliferation of stained bacteria within lettuce leaf explants post-infiltration.

Circles and squares represent stained and unstained bacteria, respectively. Values are given as means with error bars representing 1 standard deviation. $n = 5$.

and unstained treatments ($P = 0.75$). Plated homogenates from lettuce leaf explants infiltrated with stained *A. tumefaciens* revealed bacterial growth within leaf tissue following infiltration (Figure 4). Levels of bacteria within leaf explants increased significantly ($P < 0.0001$) over the first 3 days postinfiltration, with final bacteria levels approximately five-fold greater than initial levels immediately following infiltration. Proliferation data from unstained bacteria in leaf tissue indicated that staining was not detrimental to bacterial growth *in planta*.

Stained and unstained *A. tumefaciens* were infiltrated into lettuce leaf tissue and *in planta* transient expression of the GUS transgene was measured via histochemical stain. Leaf disk area exhibiting GUS activity per unit average volume of infiltrated *A. tumefaciens* was $4.20 \pm 1.03 \text{ mm}^2/\mu\text{L}$ for leaves infiltrated with labeled bacteria and $4.03 \pm 1.26 \text{ mm}^2/\mu\text{L}$ for leaves infiltrated with unlabeled bacteria (± 1 standard error of the mean, $n = 10$) (Figure 5). There was no significant difference in GUS activity between leaves infiltrated with stained or unstained bacteria ($P = 0.91$), suggesting that staining does not significantly affect agroinfiltration of lettuce. No GUS activity was detected in leaves infiltrated with water (control).

Imaging of labeled *A. tumefaciens* within leaf tissues

Sections of leaf explants infiltrated with *A. tumefaciens* labeled with Syto 16 were imaged via fluorescent confocal microscopy to visualize stained bacteria against a leaf background. In negative control leaves infiltrated with only water, fluorescent signals were observed with intensities ranging approximately 210–230 (12-bit scale). These signals corresponded primarily to chloroplasts and the epidermis (Figure 6A,C,E). As chloroplasts often line the interior surface of plant cells,²⁸ chloroplast autofluorescence could be used in conjunction with brightfield images to delineate mesophyll cells at the focal plane within a given field of view. In leaves infiltrated with stained bacteria, localized fluorescent contrasts around the periphery of certain plant cells were observed immediately following infiltration (Figure 6B,D,F). These localized fluorescence signals exhibited greater intensities than autofluorescence observed in negative

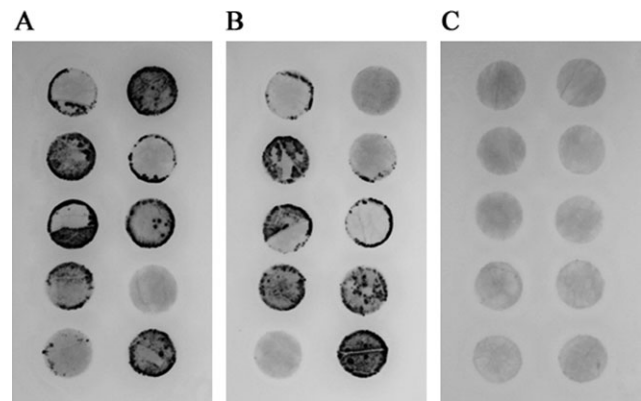


Figure 5. Infiltrated lettuce explants treated with histochemical stain to elucidate areas of recombinant GUS activity at 72 h postinfiltration.

Leaf explants were infiltrated with Syto 16-stained *A. tumefaciens* (A), unstained *A. tumefaciens* (B), or water (C).

controls and were consistent with the size of bacteria, suggesting they represent stained *A. tumefaciens*. *A. tumefaciens* were primarily observed attached to mesophyll cells. Few bacteria were detected attached to epidermal cells and none were found attached to vascular tissues.

Bacterial signals could be detected at multiple tissue depths within an infection site (Figure 7). Bacterial signals remained primarily associated with surfaces of mesophyll cells across all depths observed. The depth limit for detecting bacterial signals within leaf tissue varied with tissue type. Bacterial signals were more difficult to detect at greater depths in palisade mesophyll relative to less dense spongy mesophyll. Bacterial signals could be consistently detected down to $20 \mu\text{m}$ within leaf tissue for both types of mesophyll. Attached bacteria per unit imaging area could be quantified using image processing tools as outlined in the materials and methods section.

The number of signals representing attached bacteria at infection sites did not change significantly over the first 24 h following infiltration. After 24 h postinfiltration, signals decreased over the next 48 h following a linear trend (Figure 8). At 72 h postinfiltration, signal density was $\sim 15\%$ of that observed immediately following infiltration. Over the same time period, fluorescent signals did not develop in nuclei of plant cells, suggesting no transfer of nucleic acid stain to plant cells as a result of T-strand transfer.

Discussion

To develop a method for visualizing *A. tumefaciens* against a leaf background, the autofluorescent properties of leaf tissue were studied using pairings of excitation and emission wavelengths corresponding to common fluorophores. Of the pairings examined, exciting with 480/30 nm light and detecting emitted light at 535/40 nm elicited the lowest autofluorescent signal in leaves. On the basis of these results, the fluorophore label for staining *A. tumefaciens* was selected to maximize fluorescence contrast against leaf tissue autofluorescence. Three different fluorescent stains, all with fluorescence at the described optimal excitation and emission wavelengths, representing dsDNA, surface protein, and cytoplasmic labeling, were tested in *A. tumefaciens*. Of the three

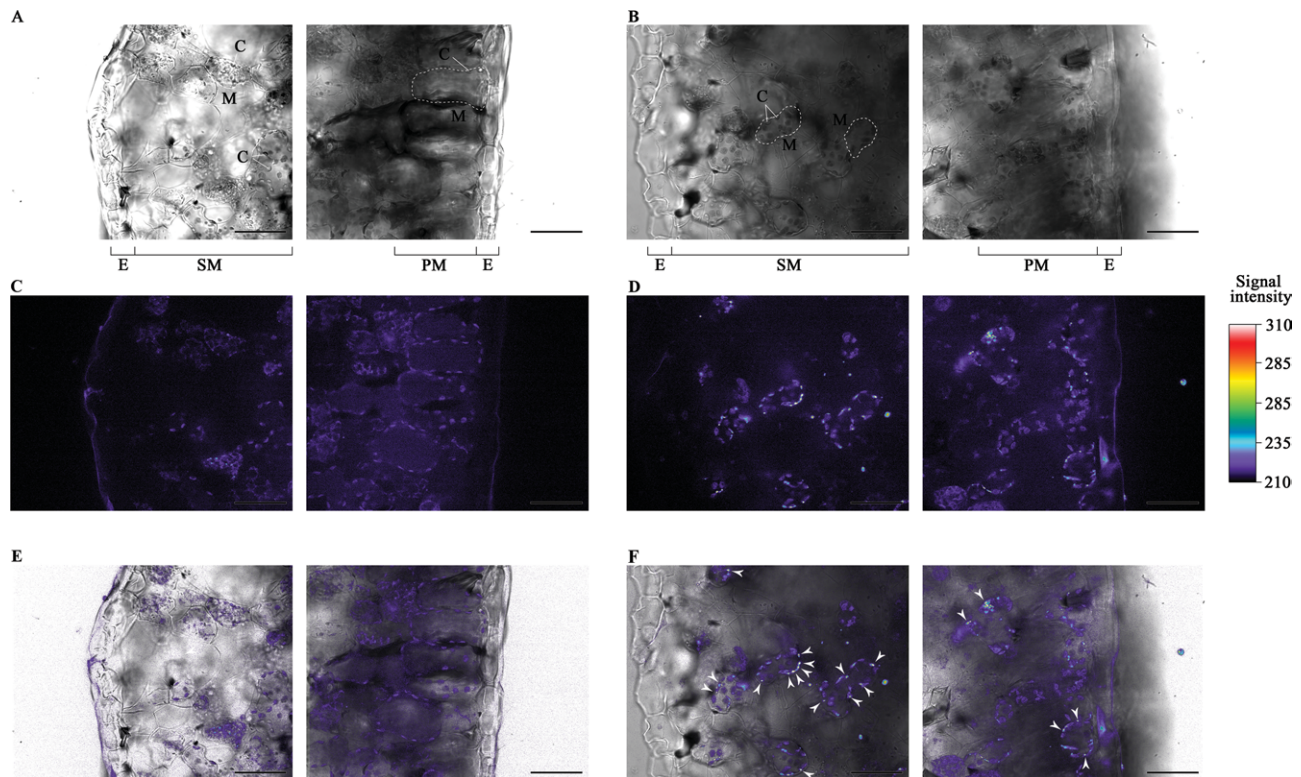


Figure 6. Representative images of lettuce leaf sections following infiltration with water (A, C, E) or Syto 16-stained *Agrobacterium tumefaciens* (B, D, F).

Images represent a transverse view of a leaf section with the abaxial side presented on the left and adjacent adaxial side on the right. Images were obtained in brightfield (A, B) and fluorescent confocal (C, D) modes. Fluorescent micrographs are given as pseudocolor images with signals scaled from 210 to 310 (12-bit). Fluorescent signals were overlaid onto corresponding brightfield images (E, F). Arrows denote examples of signals from attached *A. tumefaciens*. Scale bars represent 40 μm . E, epidermis; SM, spongy mesophyll; PM, palisade mesophyll; M, example of mesophyll cell; C, example of chloroplast.

staining modalities, the dsDNA dye Syto 16 green fluorescent nucleic acid stain yielded the greatest signal intensity in labeled bacteria. Stain concentration could be varied to control signal intensity in stained bacteria, demonstrating that signal intensity can be tuned for detection of bacteria in various systems. Moreover, staining with Syto 16 did not significantly impact the viability of the bacteria or their ability to transfer T-DNA to host plant cells. In light of this, the binding of Syto 16 to dsDNA through intercalation may be sufficiently reversible as to not interfere with DNA replication, gene expression, and virulence protein association with T-DNA.

Staining with 10 μM Syto 16 provided sufficient contrast for in situ imaging in leaves. This concentration yielded approximately half the maximum theoretical signal intensity according to stain concentration data, suggesting that higher stain concentrations could be used to increase signal intensity in systems where higher sensitivity is desired. *A. tumefaciens* stained with Syto 16 could be distinguished against a leaf background after infiltration into the leaf interior. Brightfield images and chlorophyll autofluorescence in confocal micrographs provided general delineation of plant cells in leaf sections. Bacterial signals were only observed in areas where plant cells were present. These observations suggest that the bacteria were attached to plant cells and not floating in the apoplast. Signal region sizes were consistent with the size of single bacteria, suggesting that individual bacteria attached to plant cells rather than clumps of bacteria. Bacterial attachment was observed in leaves immediately

following infiltration. The rapid attachment seen in this study is consistent with observations made on *A. tumefaciens* binding to potato tuber disks,²⁹ which show that binding of the plant tissue is saturated within one hour of exposure to *A. tumefaciens*.

Bacteria were primarily found to be attached to mesophyll cells. This agrees with transgene expression studies in *Arabidopsis* cotyledon explants, where only mesophyll cells were found to be successfully transformed following incubation with *A. tumefaciens*³⁰. While other studies have reported agroinfiltration of *Arabidopsis* epidermal cells,^{3,4} these studies subjected leaf tissues to surfactant during infiltration of *A. tumefaciens*, which may have altered bacterial interactions with the epidermis due to disruption of the cuticle. As a result, the data presented here suggest that staining does not affect the attachment behavior of *A. tumefaciens*, as attachment distributions are consistent with known transgene expression patterns in leaves agroinfiltrated under similar conditions.³⁰

Fluorescent signals from *A. tumefaciens* attached to leaf cells could be quantified at multiple depths within an infection site using fluorescent confocal microscopy. The ability of fluorescent confocal microscopy to isolate signals from the focal plane while blocking many of the contaminating background signals (i.e., out of focus light) allows bacteria to be counted across a precise volume of leaf tissue, providing measurements of attachment density that are difficult to achieve with light or electron microscopy. However, concentration measurements of attached bacteria obtained using the

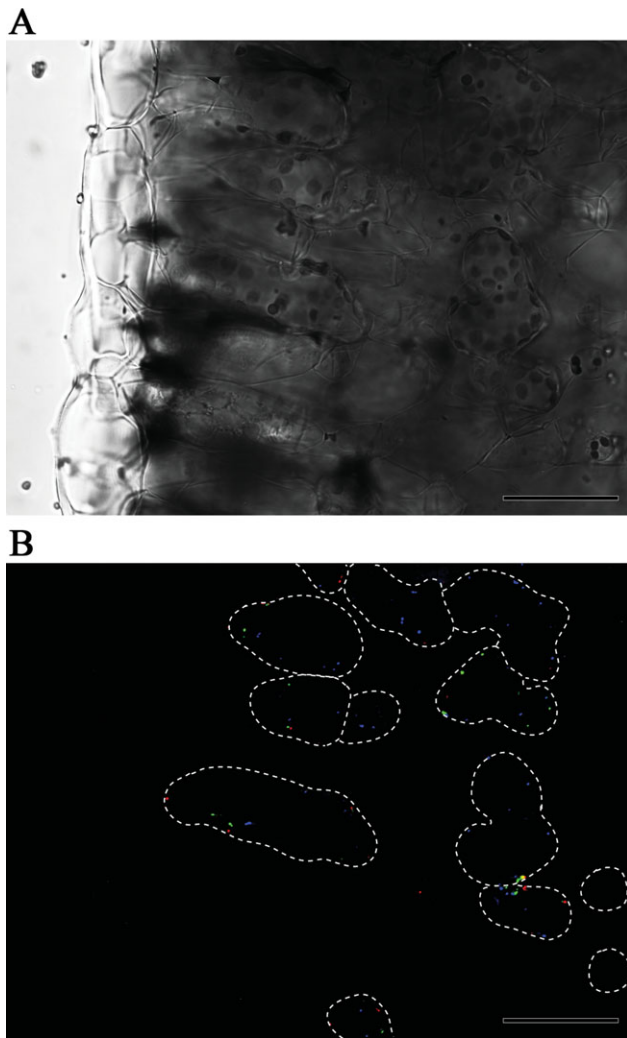


Figure 7. Representative images of depthwise detection of Syto 16-stained *Agrobacterium tumefaciens* following infiltration into lettuce leaf tissue.

The field of view depicts a transverse view of spongy mesophyll and associated epidermis in brightfield (A) and fluorescent confocal (B) modes. In fluorescent confocal micrographs, blue, green, and red signals represent signals at 0, 10, and 20 μm relative depth within the infection site. Fluorescent signals from the three imaged tissue depths were scaled from 240 to 270 (12-bit) to isolate signals from attached bacteria. Scale bars represent 40 μm . Dashed lines represent the approximate projection of mesophyll cells captured across the sampling depth, as determined from brightfield images and chloroplast autofluorescence.

described methods likely represent a fraction of total bacteria attached a given infection site. This stems from the 10 μm depth sampling interval used. This interval was chosen to prevent bacteria from appearing in multiple images across the sampling depth, which would lead to repeat counting of these cells. However, bacteria likely exist between the imaged focal planes and were not included in calculations of attachment density. Greater resolution in measuring concentration of attached bacteria could be achieved by decreasing the depth sampling interval while using 3D reconstruction tools found in many image analysis programs to track objects spanning multiple focal planes.

The number of bacterial signals in infiltrated lettuce leaf explants was found to decrease over 72 h following infiltration. Given that signal intensity was stable in bacteria stored

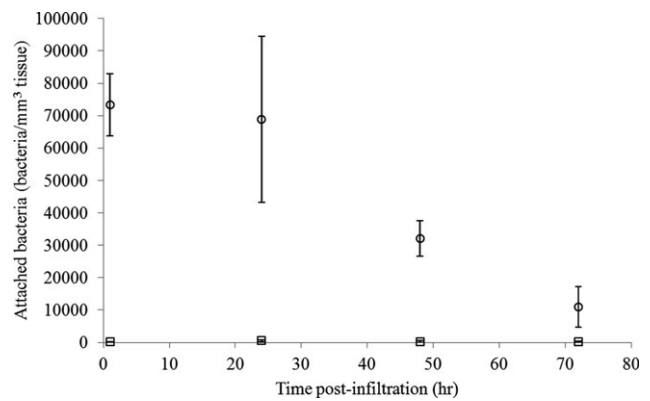


Figure 8. Attached *Agrobacterium tumefaciens* versus time post-infiltration in lettuce leaf explants infiltrated with Syto16-stained *A. tumefaciens* or water.

Circles and squares represent data from bacterial and water infiltrations, respectively. Values are given as means with error bars representing 1 standard error of the mean. $n = 3$.

in water under similar incubation conditions, it is unlikely that the decrease in observed attached bacteria over time results from degradation or bleaching of the stain. Rather, the observed decrease in signal intensity over time in bacteria cultured after staining and demonstrated proliferation of stained bacteria within leaf tissue following infiltration suggest that the nucleic stain becomes diluted among daughter cells until it is undetectable. As a result, Syto 16-staining may be most useful for observing attachment behavior within the early doubling times of *A. tumefaciens*, with the exact number of doubling times being dependent on the stain concentration used. However, prior research into *A. tumefaciens* attachment kinetics revealed that bacterial adhesion to plant cells occurs within hours of exposure to plant tissue for a variety of plant hosts^{31–33}. Moreover, it has been reported that transformation of plant tissue occurs within 8 hours of bacterial exposure³². These results suggest that the first 24 hours post-infiltration, where bacterial signal densities were observed to be stable in infiltrated leaves, are likely sufficient for studying bacterial attachment as it relates to agroinfiltration.

While this method was developed using lettuce as a model expression host, it can be reasonably assumed that it is applicable to other plant expression hosts, such as *Nicotiana benthamiana*. Although other plant systems may present varying levels of autofluorescence, data presented here demonstrate that stain concentration can be altered to control bacterial signal intensity in order to enhance contrast against leaf autofluorescence. Moreover, Syto 16 has previously been used to stain a variety of gram-positive and gram-negative bacteria^{34,35}. This suggests that the imaging technique can likely be extended to study distribution and attachment of other bacteria relevant to plant systems, such as *Agrobacterium rhizogenes*, *Pseudomonas syringae*, and *Escherichia coli*.

Conclusions

In this study, the usefulness of fluorescent confocal microscopy for mapping the distribution of and quantifying levels of fluorescently stained *A. tumefaciens* in lettuce leaf tissue with cellular resolution was demonstrated. Fluorescent nucleic acid staining of *A. tumefaciens* offers a method for rapidly creating fluorescent *A. tumefaciens* compared with generating strains expressing fluorescent proteins.

Furthermore, bacterial signal intensity is easily controlled through stain concentration compared to altering gene expression in recombinant bacteria expressing fluorescent proteins. Staining does not significantly affect bacterial viability or virulence, permitting study of native bacterial behavior downstream of attachment observations. This method can be used in conjunction with traditional techniques for gauging *A. tumefaciens* attachment and will enhance mapping and quantification of bacterial attachment to leaf cells. In particular, it will benefit studies seeking to elucidate three-dimensional *A. tumefaciens* attachment in the complex ultrastructure of leaf tissues, where other microscopy approaches encounter difficulties. This work promotes further research into *A. tumefaciens* attachment to host plants, particularly regarding how various mutations and environmental conditions affect attachment behavior, how infiltration processes like vacuum infiltration influence bacterial attachment to host leaf tissues, and how attachment relates to agroinfiltration of plant tissues.

Acknowledgments

The authors thank Judy Jernstedt, Department of Plant Sciences, UC Davis, for assistance with leaf tissue sectioning. This material is based upon work supported by the National Science Foundation under Grant No. DGE-0653984.

Literature Cited

- Fischer R, Stoger E, Schillberg S, Christou P, Twyman R. Plant-based production of biopharmaceuticals. *Curr Opin Plant Biol.* 2004;7:152–158.
- Rybicki E. Plant-made vaccines for humans and animals. *Plant Biotechnol J.* 2011;8:620–637.
- Marion J, Bach L, Bellec Y, Meyer C, Gissot L, Faure J-D. Systematic analysis of protein subcellular localization and interaction using high-throughput transient transformation of *Arabidopsis* seedlings. *Plant J.* 2008;56:169–179.
- Li J-F, Park E, Arnim Av, Nebenführ A. The FAST technique: a simplified *Agrobacterium*-based transformation method for transient gene expression analysis in seedlings of *Arabidopsis* and other plant species. *Plant Methods.* 2009;5:6.
- Lippincott B, Whatley M, Lippincott J. Tumor induction by *Agrobacterium* involves attachment of the bacterium to a site on the host plant cell wall. *Plant Physiol.* 1977;59:388–390.
- Bechtold N, Pelletier G. In planta *Agrobacterium*-mediated transformation of adult *Arabidopsis thaliana* plants by vacuum infiltration. *Methods Mol Bio.* 1998;82:259–266.
- Simmons C, VanderGheynst J, Upadhyaya S. A model of *Agrobacterium tumefaciens* vacuum infiltration into harvested leaf tissue and subsequent in planta transgene transient expression. *Biotechnol Bioeng.* 2009;102:965–970.
- Gelvin S. Plant proteins involved with *Agrobacterium*-mediated genetic transformation. *Annu Rev Phytopathol.* 2010;48:45–68.
- Tonlinson A, Fuqua C. Regulation of polar surface attachment in *Agrobacterium tumefaciens*. *Curr Opin Microbiol.* 2009;12:708–714.
- Douglas C, Halperin W, Nester E. *Agrobacterium tumefaciens* mutants affected in attachment to plant cells. *J Bacteriol.* 1982;152:1265–1275.
- Matthysse A, Wyman P, Holmes K. Plasmid-dependant attachment of *Agrobacterium tumefaciens* to plant tissue culture cells. *Infect Immun.* 1978;22:516–522.
- Matthysse A. Characterization of non-attaching mutants of *Agrobacterium tumefaciens*. *J Bacteriol.* 1987;169:313–323.
- Reuhs B, Kim J, Matthysse A. Attachment of *Agrobacterium tumefaciens* to carrot cells and *Arabidopsis* wound sites is correlated with the presence of a cell-associated, acidic polysaccharide. *J Bacteriol.* 1997;179:5372–5379.
- Graves A, Goldman S, Banks S, Graves A. Scanning electron microscope studies of *Agrobacterium tumefaciens* attachment to *Zea mays*, *Gladiolus* sp., and *Triticum aestivum*. *J Bacteriol.* 1988;170:2395–2400.
- Matthysse A, Marry M, Krall L, et al. The effect of cellulose overproduction on binding and biofilm formation on roots by *Agrobacterium tumefaciens*. *Mol Plant Microbe In.* 2005;18:1002–1010.
- Clauce-Couple H, Chateau S, Ducrocq C, et al. Role of vitronectin-like protein in *Agrobacterium* attachment and transformation of *Arabidopsis* cells. *Protoplasma.* 2008;234:65–75.
- Verma A, Nain V, Kumari C, Singh S, Narasu M, Kumar P. Tissue specific response of *Agrobacterium tumefaciens* attachment to *Sorghum bicolor* (L) Moench. *Physiol Mol Biol Plants.* 2008;14:307–313.
- Matthysse A. Initial interactions of *Agrobacterium tumefaciens* with plant host cells. *Crit Rev Microbiol.* 1986;13:281–307.
- Finer K, Finer J. Use of *Agrobacterium* expressing green fluorescent protein to evaluate colonization of sonication-assisted *Agrobacterium*-mediated transformation-treated soybean cotyledons. *Lett Appl Microbiol.* 2000;30:406–410.
- Ramey B, Koutsoudis M, Bodman Sv, Fuqua C. Biofilm formation in plant-microbe associations. *Curr Opin Microbiol.* 2004;7:602–609.
- Georgio Pd, Bird D, Prairie Y, Planas D. Flow cytometric determination of bacterial abundance in lake plankton with the green nucleic acid stain SYTO 13. *Limnol Oceanogr.* 1996;41:783–789.
- Guindulain T, Comas J, Vives-Rego J. Use of nucleic acid dyes SYTO-13, TOTO-1, and YOYO-1 in the study of *Escherichia coli* and marine prokaryotic populations by flow cytometry. *Appl Environ Microb.* 1997;63:4608–4611.
- Florian B, Noël N, Sand W. Visualization of initial attachment of bioleaching bacteria using combined atomic force and epifluorescence microscopy. *Miner Eng.* 2010;23:532–535.
- Khan M, Pyle B, Camper A. Specific and rapid enumeration of viable but nonculturable and viable-culturable Gram-negative bacteria by using flow cytometry. *Appl Environ Microb.* 2010;76:5088–5096.
- Sjollema J, Rustema-Abbing M, Mei Hvd, Busscher H. Generalized relationship between numbers of bacteria and their viability in biofilms. *Appl Environ Microb.* 2011;77:5027–5029.
- Wroblewski T, Tomczak A, Michelmor R. Optimization of *Agrobacterium*-mediated transient assays of gene expression in lettuce, tomato and *Arabidopsis*. *Plant Biotech J.* 2005;3:259–273.
- Joh L, Wroblewski T, Ewing N, VanderGheynst J. High-level transient expression of recombinant protein in lettuce. *Biotechnol Bioeng.* 2005;91:861–871.
- Haupt W. Role of light in chloroplast movement. *BioScience.* 1973;23:289–296.
- Kluepfel D, Pueppke S. Adsorption of *Agrobacterium tumefaciens* to susceptible potato tissues: a physisorption process. *Appl Environ Microb.* 1986;51:1130–1132.
- Sangwan R, Bourgeois Y, Brown S, Vasseur G, Sangwan-Norreel B. Characterization of competent cells and early events of *Agrobacterium*-mediated genetic transformation in *Arabidopsis thaliana*. *Planta.* 1992;188:439–456.
- Neff N, Binns A. *Agrobacterium tumefaciens* interaction with suspension-cultured tomato cells. *Plant Physiol.* 1985;77:35–42.
- Sykes L, Matthysse A. Time required for tumor induction by *Agrobacterium tumefaciens*. *Appl Environ Microb.* 1986;52:597–598.
- Matthysse A, McMahan S. The effect of the *Agrobacterium tumefaciens* attR mutation on attachment and root colonization differs between legumes and other dicots. *Appl Environ Microb.* 2001;67:1070–1075.
- Lomander A, Schreuders P, Russek-Cohen E, Ali L. Evaluation of chlorines' impact on biofilms on scratched stainless steel surfaces. *Bioresource Technol.* 2004;94:275–283.
- Wang J, Chen YP, Yao K, et al. Robust antimicrobial compounds and polymers derived from natural resin acids. *Chem Commun.* 2012;48:916–918.